Cytocompatible, Photoreversible, and Self-Healing Hydrogels for Regulating Bone Marrow Stromal Cell Differentiation

Lianlian Yu, Kaige Xu, Liangpeng Ge, Wenbing Wan, Ali Darabi, Malcolm Xing,* Wen Zhong*

Photo-crosslinking and self-healing have received considerable attention for the design of intelligent materials. A novel photostimulated, self-healing, and cytocompatible hydrogel system is reported. A coumarin methacrylate crosslinker is synthesized to modify the polyacrylamide-based hydrogels. With the [2+2] cyclo-addition of coumarin moieties, the hydrogels exhibit excellent self-healing capacity when they are exposed to light with wavelengths at 280 and 365 nm, respectively. To enhance cell compatibility, a poly (amidoamine) crosslinker is also synthesized. Variations in light exposure times and irradiation wavelengths are found to alter the self-healing property of the hydrogels. The hydrogels are shown to induce a regular cellular pattern. The hydrogels are used to regulate bone marrow stromal cells differentiation. The relative mRNA expressions are recorded to monitor the osteogenic differentiation of the cells.

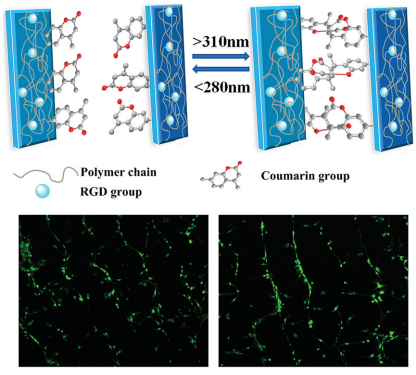

1. Introduction

The phenomenon of self-healing exists widely in living organisms, from blood clotting to skin repair. This special biological process helps living organisms to restore their integrity and prolong their lifespan.[1] Mimicking such a natural healing feature, materials with the capacity of self-repairing after being damaged are highly desirable in biomedical applications. For example, if applied in tissue engineering, a self-healing scaffold can self-repair the cracks or damages that can occur during or after implantation, and consequently, minimize the needs of further procedures and enhance the efficacy of the treatment.

A variety of smart materials that have self-healing capacities have been developed based on various strategies,[2–9] including the photosensitive self-healing polymers.[10–12] Coumarins are a class of molecules including hundreds of derivatives. Their photosensitivity was discovered one century ago.[13] Coumarin-containing polymers have been well studied and widely applied in many fields, including biochemicals, organic–inorganic hybrid materials, liquid crystalline materials, electro-optical materials, and light harvesting/energy transferring materials.[14–21] In addition, their photocleavage behavior and reversible photocrosslinking property have been widely investigated.[22–25]

L. Yu, Prof. W. Zhong
Department of Biosystem Engineering
University of Manitoba
Winnipeg MB R3T 2N2, Canada
E-mail: wen.zhong@umanitoba.ca
K. Xu, L. Ge, W. Wan, A. Darabi, Prof. M. Xing
Department of Mechanical Engineering
University of Manitoba
Winnipeg MB R3T 2N2, Canada
E-mail: malcolm.xing@umanitoba.ca
Prof. M. Xing
Manitoba Institute of Child Health
Winnipeg MB R3T 2N2, Canada
Prof. M. Xing
Department of Biochemistry and Medical Genetics
University of Manitoba
Winnipeg MB R3T 2N2, Canada

Macromol. Biosci. **2016**, DOI: 10.1002/mabi.201500457

Recently, there have also been studies on self-healing materials containing coumarin compounds.[26] However, cell-compatibility of these materials has been a concern due to the usage of such crosslinkers as formaldehyde.[27] It is still a great challenge to fabricate macromolecular materials with both superior self-healing and cytocompatible performances. The [2+2] cycloaddition of a couple of coumarin moieties forms a cyclobutane ring under a UVA (long wave UV) irradiation (320–400 nm). Being exposed to an UVC (short wave UV) irradiation (200–280 nm), on the other hand, the coumarin photodimers are cleaved to release the original coumarin moieties (Figure 6). Polymers containing coumarin structural parts, therefore, exhibit fast photoresponsibility and effective photoreversibility at different wavelengths of UV light. Poly (amidoamine)s are a family of synthetic polymers containing tertiary amino and amido groups regularly arranged along their polymer chain.[28–30] They are obtained by Michael-type polyaddition of primary or secondary amines to bis-acrylamides. By using such functionalized monomers as aminocarbohydrate derivatives, PAAs can be easily modified to incorporate such side substituents as additional tertiary amino groups, carboxyl groups, hydroxyl groups, and allyl groups.[31] However, for materials used in biological application, biocompatibility is another important issue. Despite of their very promising properties, synthetic hydrogels are characterized by poor cell adhesion.[32] Efforts have been made to improve biocompatibility and cell adhesion of hydrogels. For example, polycations such as poly(L-lysine) was used to enhance the cytocompatibility of hydrogels.[33,34] 4-aminobutyl guanidine or agmatine was also introduced to build a functional amphoteric repeating unit with a structure similar to the tripeptidearginin-glycin-aspartic acid (RGD), which presents in extra cellular matrix (ECM).[31] PAAs hydrogels incorporating RGD-mimicking units have been shown to have a superior cell adhesion capability as compared to plain amphoteric PAAs.[35,36]

Based on the aforementioned, both cell-compatibility and self-healing capacity might be achieved by taking advantages of the photoresponsive behavior of coumarin and RGD-mimicking units in the PAA, as it will be developed and discussed in this work. Most existing work in this area focuses more on the reaction mechanisms of the materials than on the biological applications of coumarin. In addition, there has been no report on self-healing macrohydrogels containing coumarin derivatives with the feature of reversible photo-crosslinking and cell attachment.

2. Experimental Section

2.1. Materials

2-Bromo-2-methylpropionyl bromide, acryloyl chloride, 7-hydroxy-4-methylcoumarin, 2-bromoethanol, triethylamine, potassium carbonate, ethanol, ether, anhydrous sodium sulfate, dichloromethane, sodium chloride, DMSO, acrylamide, *N,N′*-methylene bis(acrylamide) (MBA), agmatine sulfate salt, 1-(2-aminoethyl)-piperozine(AEPZ), *N,N,N′,N′*-tetramethylethanediamine (TEMED), ammonium persulfate (APS), and lithium hydroxide (LiOH) were all purchased from Sigma-Aldrich without further purification. PBS (phosphate-buffered saline) 1x powder, Hoechst 33342, BODIPY FL phallacidin, To-Pro-3 iodide and Live-Cell staining kit were all purchased from Invitrogen. The 3-(4,5-dimethyl thiazolyl-2)-2,5-diphenyltetrazolium bromide (MTT) cell viability assay kits were from Biotium Inc. (Hayward, CA). O.C.T. compounds were purchased from V.W.R FITC fluorescence dye and RT-PCR kit was purchased from Thermo Scientific. UV exposure power was 16 mw cm^{-2}.

2.2. Synthesis of Coumarin Methacrylate (CMA) Crosslinker

The synthesis of coumarin methacrylate (CMA) crosslinker was conducted by a two-step reaction. As showed in Figure 1. First, a mixture of 7-hydroxy-4-methylcoumarin (5.0 g, 25.7 mmol), 2-bromoethanol (5.0 g, 40.0 mmol), and potassium carbonate (3.0 g, 21.7 mmol) in 50 mL of ethanol was heated under reflux for 20 h. The mixture was then cooled at rt, diluted with ether and water. The mixture was separated, and the aqueous layer was extracted with ether. The combined organic layer was dried over magnesium sulfate, followed by the removal of the solvent.

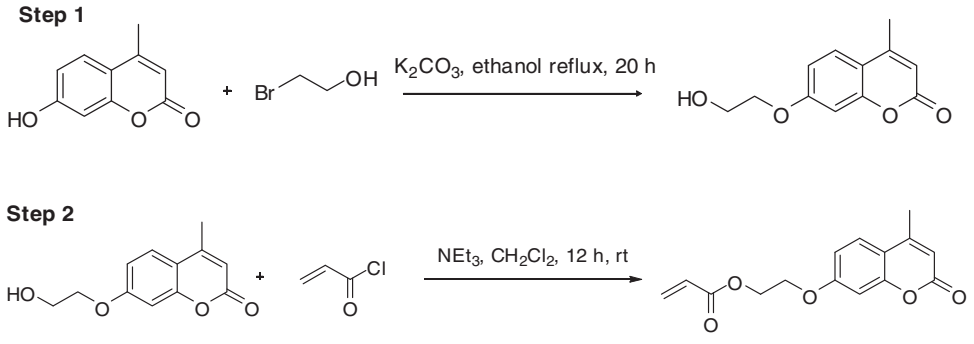

Figure 1. Schematic illustration of two-step synthesis of the CMA crosslinker.

Macromolecular Journals
Macromol. Biosci. **2016**, DOI: 10.1002/mabi.201500457

The solid obtained, was pure enough to use in the next step without further purification.

To a solution of triethylamine (5.0 g, 6.89 mL, 49.4 mmol) and 7-(2-hydroxyethoxy)-4-methylcoumarin (5.0 g, 20.14 mmol) in 80 mL of dichloromethane, was added dropwise acryloyl chloride (5.0 g, 4.48 mL, 55.24 mmol). After being stirred for 12 h at room temperature, water was added. The mixture was separated, and the aqueous layer was extracted with dichloromethane. The combined organic layer was washed with an aqueous solution of NaCl, followed by drying over anhydrous sodium sulfate and the removal of the solvent to give a solid. The crude product was recrystallized from ethanol to afford colorless powdery crystals.

2.3. Synthesis of the PAA Crosslinker

The agmatine containing poly(amidoamine) (PAA) crosslinker was synthesized via Michael-addition polymerization as shown in Figure 2. MBA (234 mg, 1.52 mmol), Agmatine (138 mg, 0.6 mmol), and AEPZ (52 mg, 0.4 mmol) were dissolved in water/methanol (v/v = 5/1, total in 5 mL) while stirring. When the solution was clear, LiOH·H2O (25.2 mg, 0.6 mmol) was added to the solution. The mixture was then gently stirred and allowed to react at 45 °C in the dark for 72 h. After reaction, the solvent was evaporated using a rotary-evaporator. The product was finally recovered by lyophylization and stored in −20 °C refrigerator for future use.

2.4. Characterization

In order to characterize the CMA crosslinker (Figure 3) and PAA crosslinker (Figure 4), 1H NMR spectra was recorded on an Advance 300 MHz spectrometer. 8 mg of crosslinker powders were dissolved in 800 μL of NMR solvent. Chemical shifts (δ) were reported in parts per million (ppm): 1H NMR (ppm, $CDCl_3$) δ for CMA crossliner: (above), 2.44 (CH_3,s, 3H), 4.28 (C***H***$_2$—O—aromatic,t, 2He), 4.55 (C***H***$_2$—OCO,t, 2Hf), 6.10 (ethylene, dd, 1Hh), 6.28 (aromatic, s, 1Ha), 6.38 (ethylene, dd, 1Hg), 6.68 (ethylene, dd, 1Hi), 7.14 (O—C_6H_3—,d, 1Hc), 7.17 (O—C_6H_3—,s, 1Hd), 7.64(O—C_6H_3—,d, 1Hb).

1H NMR (ppm) for PAA crosslinker: δ, 1.5 (H14 + H13, m, 4nH), 2.0-3.0(H2 + H5 + H7 + H9 + H10 + H11 + H12,m, 8nH), 3.17(H15, t, 2nH), 4.53 and 4.62(H1 + H6,s, (2n+2)H), 5.77 (ethylene, dd, 2H18), 6.21(ethylene, dd, 2H17), 6.225 (ethylene, dd, 2H16).

2.5. Synthesis of CMA Containing Hydrogel

Coumarin-containing hydrogel was prepared by copolymerization of acrylamide (6.2 mmol), 7-(2-methacryloyloxyethoxy)-4-methylcoumarin (0.31 mmol), PAA crosslinker (0.97 mmol) using APS (0.20 mmol), and TEMED in 1.0 mL of DMSO at 65 °C. The gel was purified by washing with large amounts of DMSO, followed by exposure to water over several hours, then repeated washing with water. To form the gel with cellular pattern, the concentrations of components were listed as in Table 1.

2.6. Evaluation of Self-Healing Capacity of the Hydrogels

2.6.1. Sample Preparation

Hydrogels for self-healing evaluations were all prepared between two glass cover slips (25 mm × 25 mm) by adding 250 μL of gel precursor solution. After gelation under 60 °C for 20 min, the cover slips were removed and then the gel was thoroughly washed with sterilized PBS solution to remove chemical residuals.

2.6.2. Confocal Laser Scanning Microscope Images of the Healing Hydrogels

The hydrogels precursor were prepared first and mixed evenly. Then 200 μL precursor was dropped onto square glass cover slips (length: 20 mm). After gelation under 65 °C, the slips with hydrogels on the surface were stained by FITC fluorescence dye. Then a crack was made through the whole thickness of the hydrogel by a blade. Fluorescence pictures before and after UV healing process (λ = 365 nm) were recorded by confocal laser scanning microscopy (CLSM) (Olympus FV1000, Japan).

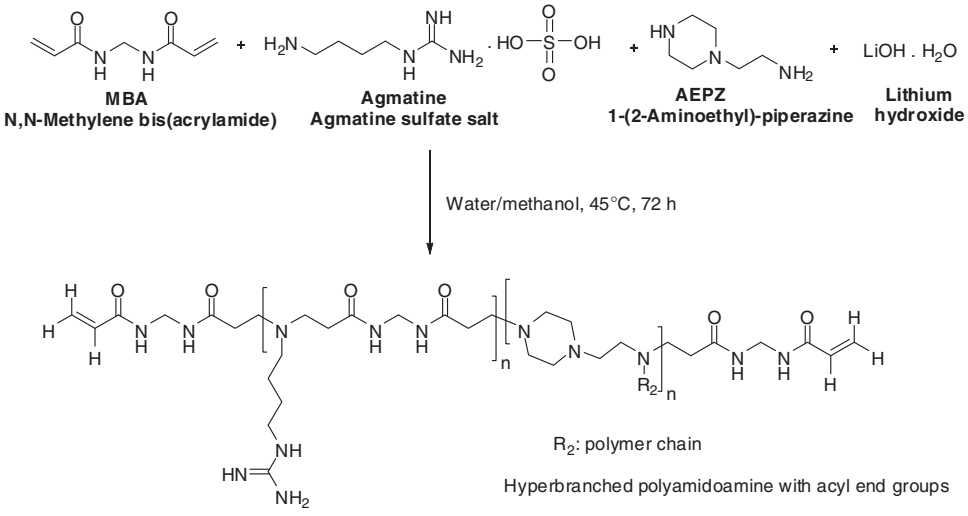

Figure 2. Schematic illustration of the preparation of the PAA crosslinker.

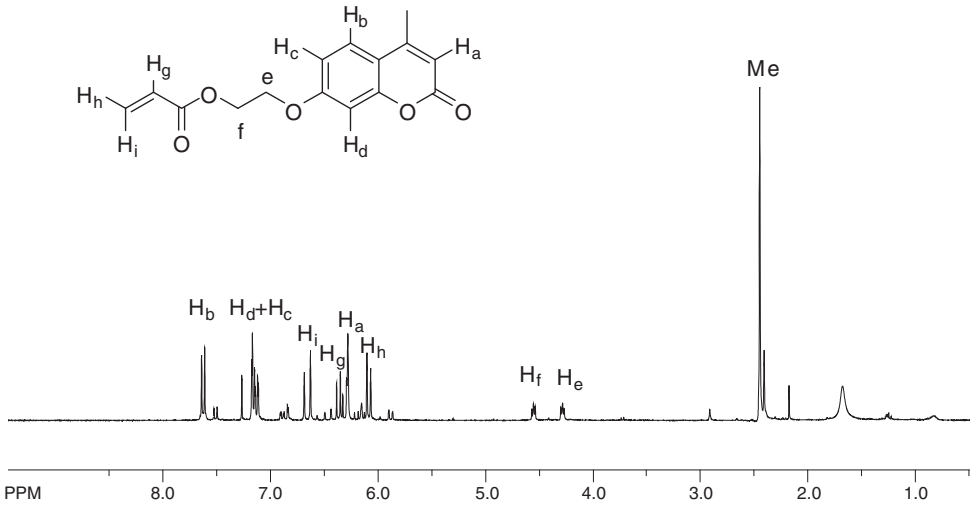

Figure 3. 1H NMR spectrum of the CMA crosslinker.

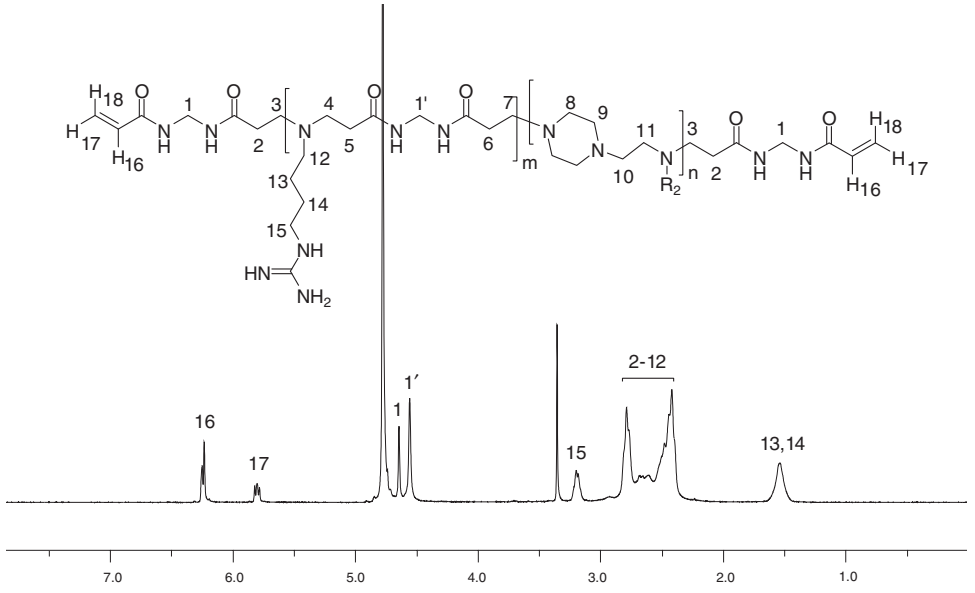

Figure 4. 1H NMR spectrum of the PAA crosslinker.

2.6.3. Tensile Tests

To further evaluate the healing capacity of the hydrogels, hydrogels containing CMA crosslinker were synthesized. Specimen of 20 mm in length, 4 mm in width and 2 mm in thickness was firstly cut by a razor. Samples were kept in alignment and intimate contact without pressure. Samples were then irradiated under UV light at the wavelength of 365 nm for 10, 20, 30 and 60 min, respectively. After the self-healing process by irradiation, the connected bars were fixed onto the INSTRON materials testing machine as showed in Figure 5. The test speed was set at 0.1 mm min^{-1}. Stress–strain curves were recorded by the

Table 1. Concentrations of components.

Whole concentration	Name	Concentration [mg mL^{-1}]	Mole	Volume [μL]
1.5 mmol mL^{-1} (97:1:2) Total 1 mL	AM	200	1.47315 mmol	523.6
	CMA	50	0.0152 mmol	87.25
	Crosslinker	30	0.0304 mmol	405.3
	APS	200	5.7 mg	28.5
	TEMED	–	2.9 mg	3.74

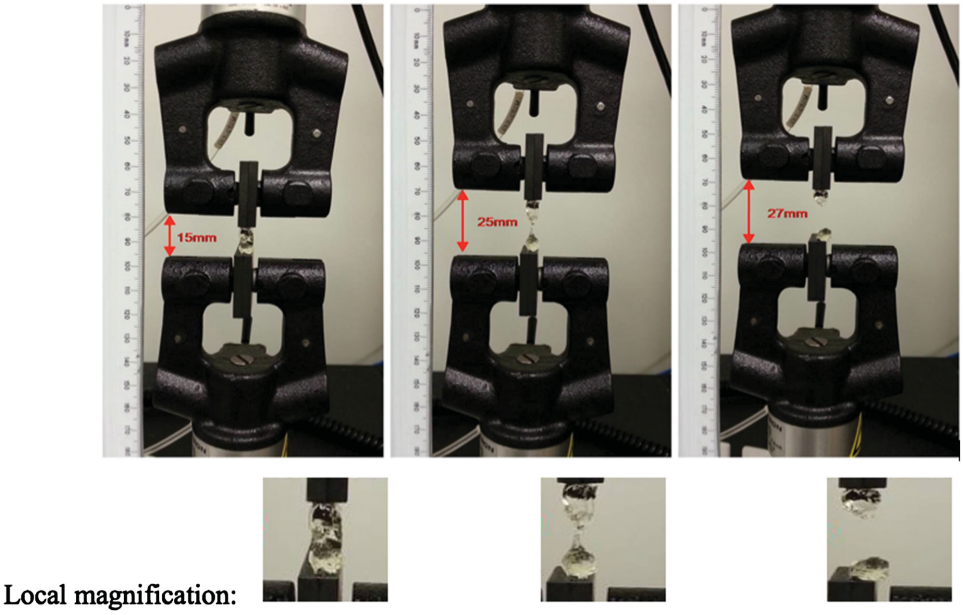

Figure 5. Images of sample test setting.

INSTRON software. All measurements were carried out at constant temperature and humidity room. The sample size of each group is 3 (n = 3). The original hydrogel samples without cut were also tested as a control to show the healing efficiency of the hydrogels.

2.6.4. Photoreversible Test

In order to verify the photoreversible property of hydrogels, UV light ($\lambda < 280$ nm) at another wavelength was applied to the mechanically bisected and then healed samples. Specifically, sample hydrogels 20 mm in length, 4 mm in width, and 2 mm in thickness were cut into two halves and subsequently allowed to heal for 30 min. The healed samples were further exposed to the UV light at the wavelength of 260 nm for 10 and 20 min, respectively. Their tensile stress and breaking elongation were again recorded on an INSTRON tester, following the procedures described in the previous section.

2.7. Swelling Test

Hydrogels were prepared in a specific size in 24-well plate as described before. Then weighed and immersed in vials which containing PBS buffer (pH = 7.4) at room temperature. At designed time intervals, the hydrogels were taken out from solution, and weighed after wiping off any visible surface moisture. The percentage amount of buffer absorbed can be calculated using the following formula

$$\text{Water}(\%) = (\text{Wt-Wo})/\text{Wo}^{*}100 \quad (1)$$

where Wt is the weight of hydrogels at weighing time and W0 is the weight of the initial weight hydrogel. In order to reduce errors, all swelling ratio results should be obtained from triplicate samples.

2.8. In Vitro Biocompatibility Test

2.8.1. Cell Culture and Growth on Hydrogel

The hydrogels precursor for cell culture were prepared first and mixed evenly. Then 100 µL precursor was dropped onto glass cover slips (diameter: 10 mm). After gelation under 37 °C, the glass cover slips were put into PBS solution for 2 h, in order to remove chemical residuals. Then the glass cover slips were taken out and irradiated under UV light in a biosafety hood for 30 min. Finally, the gels coated glass cover slips were placed in cell culture dishes (35 mm × 10 mm). Mouse bone marrow stromal cells (BMSCs from ATCC, USA) were cultured with Dulbecco's Modified Eagle's Medium (DMEM, GIBCO) supplemented with 10% fetal bovine serum (FBS, GIBCO), 1.0×10^5 UI^{-1} penicillin (Sigma) and 100 mg mL^{-1} streptomycin (Sigma) at 37 °C in 5% CO2. Live/dead staining was carried out to evaluate the cytotoxicity of hydrogels, according to a protocol from Invitrogen Inc., Canada. BMSC cultures were performed using hydrogels and stained at 24 h, 3 d, and 7 d. Images were taken by CLSM.

2.8.2. Quantitative Real-Time PCR Analysis

100 mL of BMSCs in medium at a density of 2×10^6 cells per mL was seeded onto the hydrogels for 30 min. Then, 2 mL medium were added to the disk. After 2 d, cell-encapsulating hydrogels were transferred to FBS-supplemented DMEM containing a combination of osteogenic chemical supplements: 50 mg mL^{-1} L-ascorbic acid 1-phosphate (Sigma), 10×10^{-3} M b-glycerophosphate (Sigma) and 100×10^{-6} M dexamethasone (Sigma). Gels with cells were incubated for various time points. The osteogenic medium was

Macromol. Biosci. **2016**, DOI: 10.1002/mabi.201500457

changed for every 2 d. At predetermined time intervals, the media were aspirated with the unattached cells and the wells were washed with DPBS (Dulbecco's phosphate-buffered saline). Then, cells on hydrogels were treated with liquid nitrogen and smashed. In order to validate the gene expression of osteogenic differentiation in all samples, total RNA isolation and cDNA synthesis were conducted using TRIzol and Oligo dT (Thermo Scientific, USA), according to the standard procedures. Then quantitative real-time PCR (qPCR) was performed by SYBER Green assays (Applied Biosystems, USA). Amplification conditions were as follows: hold at 95 °C for 10 min, followed by 40 cycles at 15 s at 95 °C and 1 min in 60 °C. Thermal cycling and fluorescence detection were done using the StepOnePlus real-time PCR System (Applied Biosystems, USA). The mRNA expression levels were determined relative to the GAPDH by the ΔCt method. The five gene premiers were (form 5′–3′): ALP-F: CTC CAA AAG CTC AAC ACC AAT G, ALP-R: ATT TGT CCA TCT CCA GCC G;BSP-F: CCA CAC TTT CCA CAC TCT CG, BSP-R: CGT CGC TTT CCT TCA CTT TTG; COL I–F: AAC AGT CGC TTC ACC TAC AG, COL I-R: AAT GTC CAA GGG AGC CAC; OPN-F: CTA CGA CCA TGA GAT TGG CAG, OPN-R: CAT GTG GCT ATA GGA TCT GGG; GAPDH-F: AGG TCG GTG TGA ACG GAT TTG, GAPDH-R: TGT AGA CCA TGT AGT TGA GGT CA.

3. Results and Discussions

In this work, the synthesis of a CMA crosslinker was conducted by a two-step reaction. In order to introduce an agmatine group into the *N*,*N*′-methylene bis(acrylamide), the poly(amidoamine) (PAA) crosslinker was synthesized via Michael-addition. NMR was conducted to verify the successful synthesis of both crosslinkers (Figures 1–4). Chemical structure of gels and mechanism of the self-healing process were showed in Figure 6. To endow polyacrylamide with photochemical reactivity, coumarin methacrylate plays dual-roles of both side groups and crosslinkers. It means that double bond groups have to be present on the backbone of the polymer to connect with PAA crosslinker and acrylamide. As a result, multi-functional homopolymer of polyacrylamide that contains coumarin groups and agmatine groups were synthesized.

Generally, damaged gels that contain coumarin groups showed significant self-healing feature upon the irradiation of 365 nm UV light. For the control group (gels without coumarin groups), however, the two halves cannot bind each other. With the treatment of UV light (365 nm), the results reflect the contribution of π–π^* transitions of the conjugated benzene nucleus and pyrone nucleus in 4-methylcoumarin chromophores.[37] Because the double bonds of 4-methylcoumarin gradually dimerize to form cyclobutane rings under 365 nm UV illumination, the conjugation between double bonds and phenyl groups was destructed (Figure 6). As a result, the two halves can connect together.

To evaluate the intrinsic healing behavior of coumarin-contained gels, the effect of coumarin on the healing process was further explored. A crack was made on the gel by a razor. The bisected samples were put in contact at their cut cross sections and exposed to 365 nm UV light irradiation for 30 min to allow self-healing. Confocal microscopy images (Figure 7) exhibited that the autonomic fusion of cut surface occurred after the UV treatment for 30 min, suggesting a good self-healing condition of the hydrogel.

Stress–strain tests were conducted to further investigate the mechanical properties of the healed hydrogels as compared to the original hydrogels. Samples were first cut into two halves, and then the two halves were brought into contact (Figure 8a). The bisected samples were exposed to 365 nm UV light irradiation for 10, 20, 30, and 60 min, respectively. Tensile tests were conducted to quantify the capacity of the damaged gels to restore their strength. For instance, the tensile stress of the gel which was irradiated for 60 min (200.2 ± 24.7kPa) is nearly five times as that of the gel which was only irradiated for 10 min (44.9 ± 17.2 kPa), indicating that the introduction of coumarin groups improves the self-healing performance of gels. Moreover, increasing the irradiation time gives rise to a remarkable improvement in the tensile modulus as well as in the breaking elongation. Gels which were irradiated for 10, 20, 30, and 60 min, showed the elongations at break at 21.6 ± 7.2%, 43.4 ± 5.2%, 67.7 ± 10.4%, and 96.2 ± 9.5%, respectively (Figure 8b). It can also be seen from the chats that 60 min of healing allows the cut samples restore to 88.6% of the original tensile modulus (Figure 8d), suggesting an excellent healing efficiency of the CMA-contained hydrogels.

To further confirm the photoreversibility of the hydrogels. The samples were cut and subsequently expose to 365 nm UV irradiation to allow self-healing for 30 min. The self-repaired samples were exposed to 254 nm UV irradiation for 10 and 20 min, respectively. Figure 9 shows reduced gel strengths with the increase in exposure time, which may be caused by the photocleavage of the formed cyclobutane rings under 254 nm UV irradiation.

Hydrogels are necessary for their high water content and low interfacial tension with the surrounding biological environment.[35] Understanding the role of gel properties on ECM formation is important for numerous biomedical applications.[24] Swelling property is important to evaluate the scaffold's biocompatibility. Figure 10 shows that the swelling ratio of both gels with and without CMA increased gradually with time. Hydrogels with CMA have a slightly lower swelling ratio as compared to the gels without CMA, which may be resulted from the changes in the crosslinking density.[15,35]

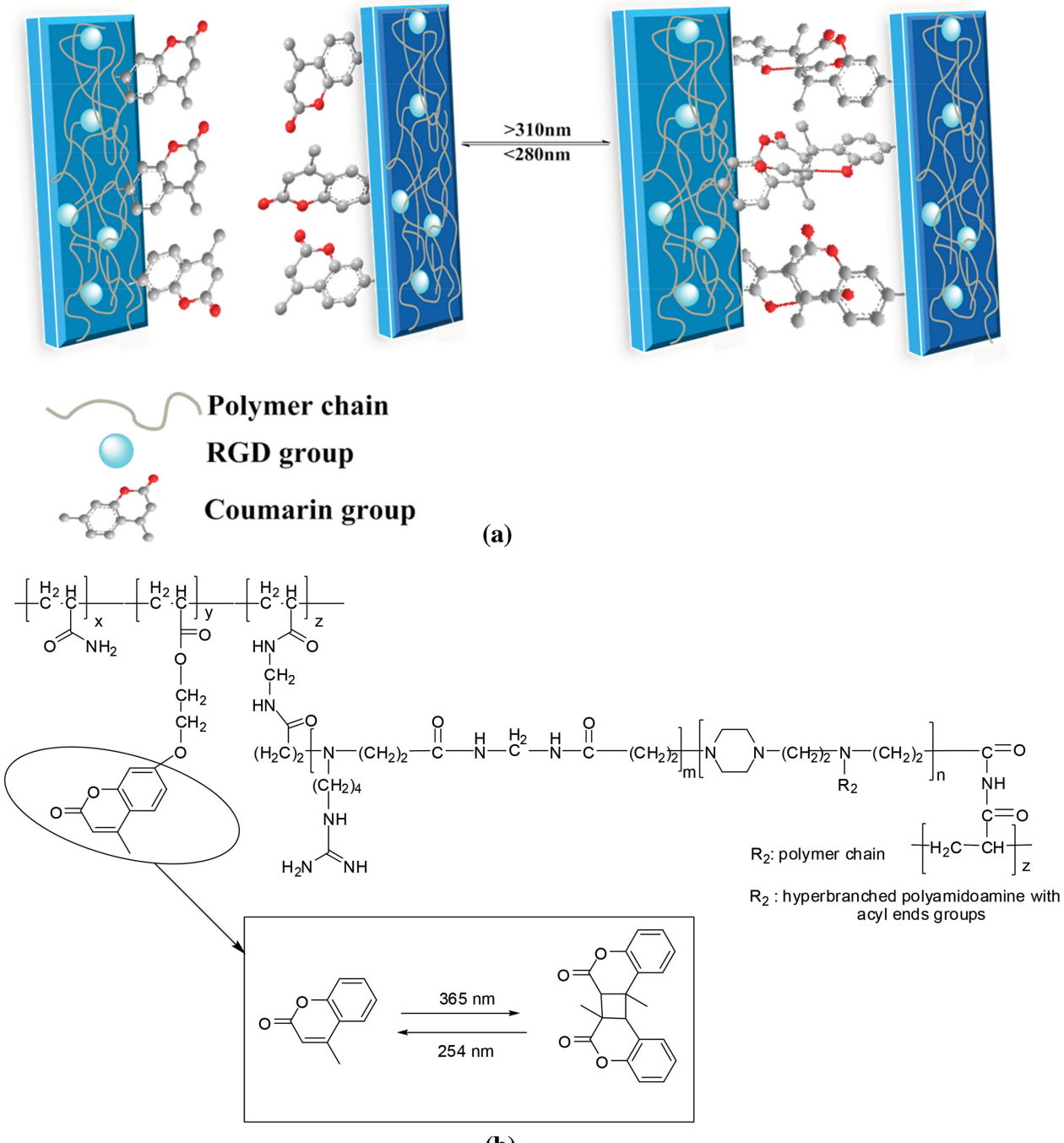

Figure 6. a) The schematic illustration of the self-healing process and b) chemical structure of the polyacrylamide gels and the photodimerization and photocleavage of coumarin side groups.

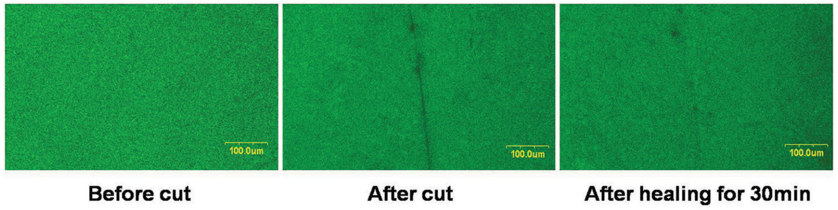

Figure 7. Fluorescence confocal microscopy images of healing process.

BMSCs were seeded onto the hydrogels. MTT assay was used to evaluate the cell viability for 24 h. Viability of cells seeded on tissue culture plates (TCPS) was normalized to 100%. As the control group, hydrogels without cells were also evaluated. As shown in Figure 11a, hydrogels with the PAA

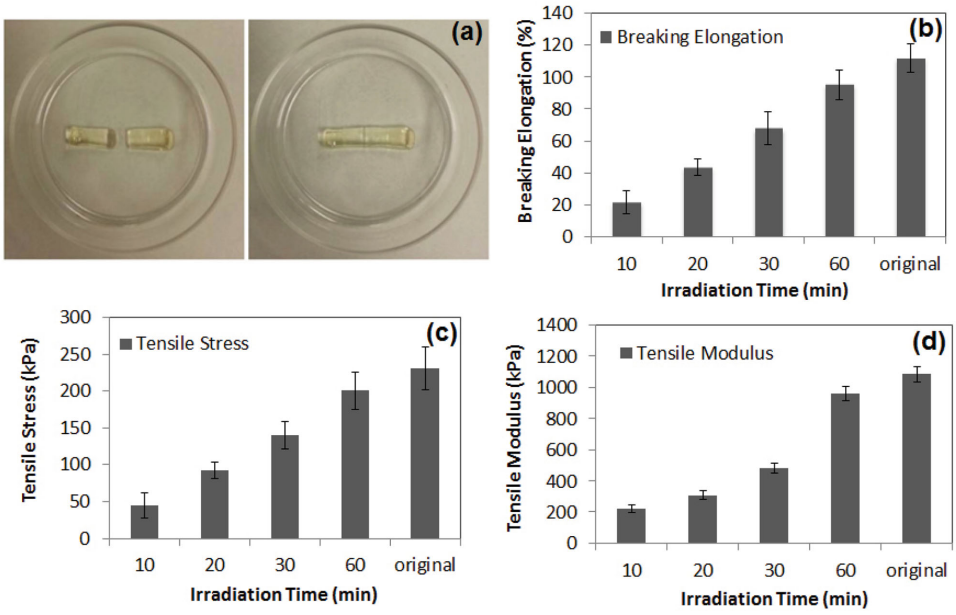

Figure 8. a) Images of sample preparation with a cut, b) breaking elongations, c) tensile stress, and d) tensile modulus of self-healed samples versus different UV irradiation time (365 nm) with 16 mw cm^{-2}, as compared to original hydrogels (n = 3).

crosslinker had high cell viability after 24 h culture. The guanidine groups from agmatine combined with the amido groups from MBA may have significantly promoted cell attachment.[36] Live/dead assay was used to evaluate the cell viability for 72 h. Hydrogels with and without the PAA crosslinker were evaluated for the cell proliferation and cell attachment. After 24 h culture, most cells were found to attach to the gels. After 72 h culture, some dead cells were found but most of them were still alive (as shown in Figure 11). The number of BMSCs increased significantly in the hydrogels that contain the PAA crosslinker. However, in the control group, a significantly lower cell density was observed, which may be due to the poor adhesion to the untreated hydrogel. The results suggest that the PAA crosslinker may improve the cell attachment to the hydrogels, therefore, endowing the self-healing gels wider applications.

More interestingly, a pattern of cell distributions was observed after the growth of the cells on the gels for 24 h. Confocal laser microscopy images demonstrate that the cells tend to align in a certain direction as show in Figure 12, when CMA and PAA crosslinker reacted with a proper ratio (Table 1), although more experiments are needed to determine the underlying mechanisms.

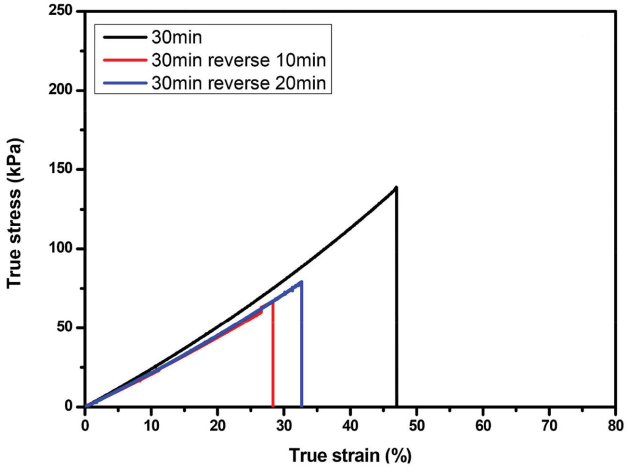

Figure 9. Stress–strain curves at different healing time with reverse conditions: 254 nm.

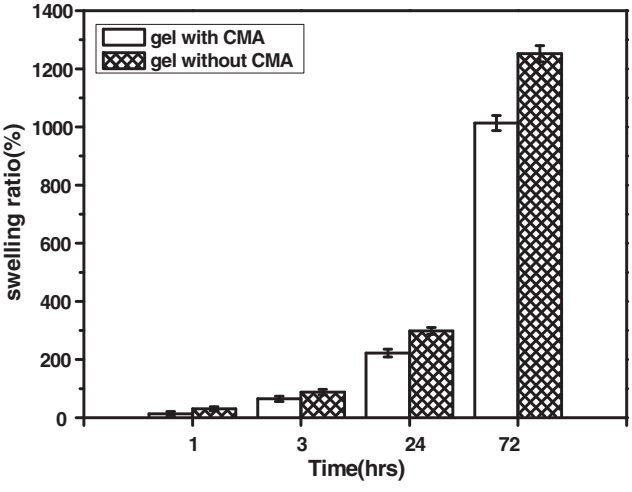

Figure 10. Swelling ratio of hydrogels with and without CMA (n = 3).

Macromolecular Journals
Macromol. Biosci. **2016**, DOI: 10.1002/mabi.201500457

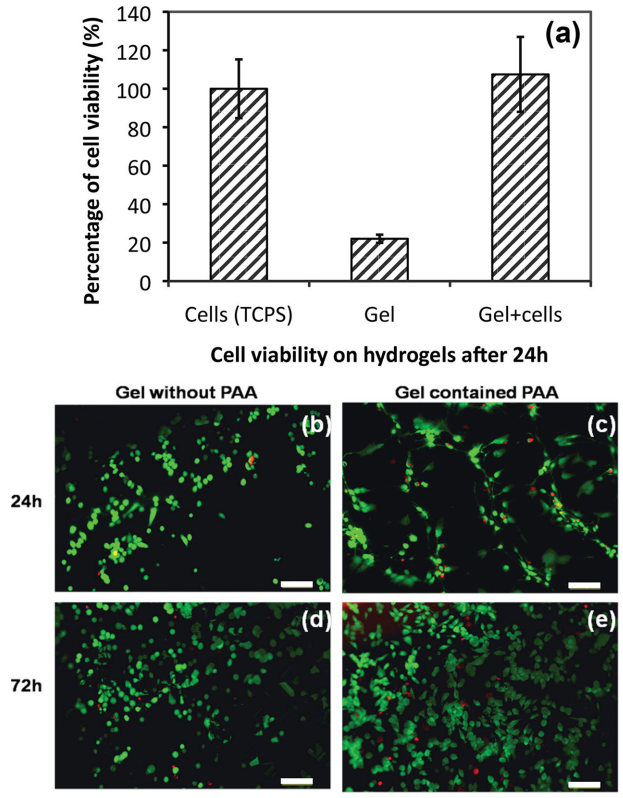

Figure 11. a) Cell viability on hydrogels after 24 h culture based on MTT assay (absorbance is normalized to 1 for the TCPS control sample) (n = 3). Live/dead assay of BMSCs cultured on b,d) hydrogels without PAA crosslinker, c,e) hydrogels containing PAA after 24 and 72 h. (Green for live cells and red for dead cells, scale: 100 μm.)

To evaluate the effects of the hydrogels on the osteogenic differentiation of BMSCs, a real time-qPCR was conducted on the BMSc-seeded hydrogels (Figure 13). Their responses to the hydrogels were recorded using the osteogenic related mRNAs for ALP, BSP, COL, and OPN. As shown in Figure 13, osteogenic gene expressions in BMSCs increased significantly after 7 d culture.

Bone sialoprotein (BSP) is an important protenforosteogenetic differentiation. It can be expressed in osteoblasts

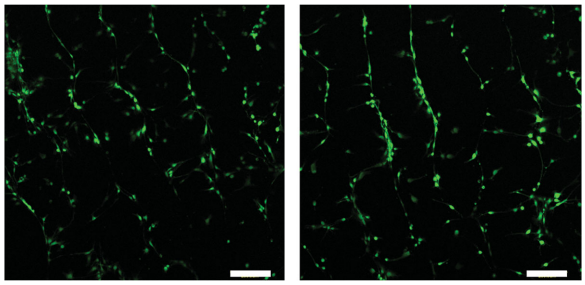

Figure 12. Confocal microscopy images of BMSC cells grown on the gel after 24 h. (Scale: 200 μm.)

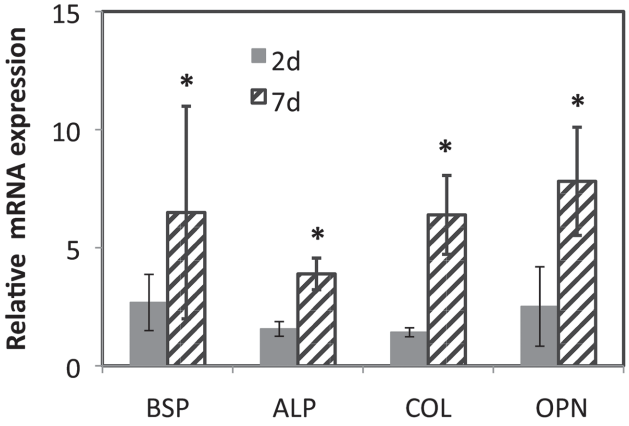

Figure 13. Real time-qPCR of osteogenic gene expression levels of mouse BMSCs cultured in vitro. Total RNA was prepared from BMSCs grown on hydrogel for 2 and 7 d. BSP, ALP, COL, OPN gene expressions were quantified using real time-qPCR methods, GAPDH was used as an internal control. Data values are expressed as mean ± SE (n = 3). "*" means $p < 0.05$ versus the groups on day 2.

or differentiated stem cells.[38] On day 2, the expression of BSP gene was found to increase and the same trend was observed on day 7 (Figure 13a). Collagen (COL) is a critical marker in the late stage of bone differentiation.[39] The expression level of COL was also found to increase with time. Osteopontin (OPN) is another important human gene which is related to osteogenesis.[40] It plays a role in organic linking component of the bone. As shown in Figure 13, the expression profiling of OPN was relatively lower than that of both BSP and COL. But the expression profiling of OPN still have a positive trend after 7 d during the osteogenetic differentiation. Alkaline phosphatase (ALP) is an enzyme that exists in all tissue in human body, which can remove the phosphate group from nucleotides or proteins. ALP may be a marker for bone metabolism: if a high level of ALP was observed, active bone tissues were generally believed to have formed.[41] The ALP expression was evaluated when BMSCs were cultured on hydrogels. The results show that the hydrogels had a high ALP expression level throughout one week (Figure 13).

3. Conclusions

In summary, we demonstrate a novel macrohydrogels with self-healing capability and biocompatibility. Coumarin derivatives are successively introduced into the polyacrylamide-based hydrogels. The reversible photodimerization and photocleavage reactivity of coumarin have been imparted to the polymer. The resultant functional gels show noticeable self-healing property after healing under 365 nm UV irradiation, ascribed to the intramolecular [2+2] photocyclo-addition reactions of coumarins. The self-healing gels also possess high mechanical

strength after healing for 60 min with stress intensity of 2×10^5 Pa and the elongation at break over 96%. More interestingly, cell attachment property was significantly improved by adding the PAA crosslinker. The development of methods and materials in this work may provide a new insight into the fabrication of novel biocompatible self-healing materials for extensive applications.

Acknowledgements: The authors would wish to thank NSERC (Natural Sciences and Engineering Research Council of Canada) for funding the present research.

Received: December 14, 2015; Revised: February 2, 2016; Published online: ; DOI: 10.1002/mabi.201500457

Keywords: crosslinker; cytocompatible; photoreversible; self-healing hydrogel

[1] C. Yu, C. F. Wang, S. Chen, *Adv. Funct. Mater.* **2013**, *24*, 1235.
[2] H. Ceylan, M. Urel, T. S. Erkal, A. B. Tekinay, A. Dana, M. O. Guler, *Adv. Funct. Mater.* **2013**, *23*, 2100.
[3] M. J. Barthel, T. Rudolph, A. Teichler, R. M. Paulus, J. Vitz, S. Hoeppener, M. D. Hager, F. H. Schacher, U. S. Schubert, *Adv. Funct. Mater.* **2013**, *23*, 4921.
[4] D. J. Lipomi, M. Vosgueritchian, B. C. Tee, S. L. Hellstrom, J. A. Lee, C. H. Fox, Z. Bao, *Nat. Nanotechnol.* **2011**, *6*, 788.
[5] T. S. Coope, U. F. Mayer, D. F. Wass, R. S. Trask, I. P. Bond, *Adv. Funct. Mater.* **2011**, *21*, 4624.
[6] M. Burnworth, L. Tang, J. R. Kumpfer, A. J. Duncan, F. L. Beyer, G. L. Fiore, S. J. Rowan, C. Weder, *Nature* **2011**, *472*, 334.
[7] J. H. Park, P. V. Braun, *Adv. Mater.* **2010**, *22*, 496.
[8] B. Ghosh, M. W. Urban, *Science* **2009**, *323*, 1458.
[9] S. R. White, N. Sottos, P. Geubelle, J. Moore, M. R. Kessler, S. Sriram, E. Brown, S. Viswanathan, *Nature* **2001**, *409*, 794.
[10] S. D. Bergman, F. Wudl, *J. Mater. Chem.* **2008**, *18*, 41.
[11] Y. Yuan, T. Yin, M. Rong, M. Zhang, *Express Polym. Lett.* **2008**, *2*, 238.
[12] Y. Yang, M. W. Urban, *Chem. Soc. Rev.* **2013**, *42*, 7446.
[13] G. Ciamician, P. Silber, *Ber. Dtsch. Chem. Ges.* **1902**, *35*, 1992.
[14] C. Graf, W. Schärtl, N. Hugenberg, *Adv. Mater.* **2000**, *12*, 1353.
[15] N. K. Mal, M. Fujiwara, Y. Tanaka, *Nature* **2003**, *421*, 350.
[16] K. Hara, T. Sato, R. Katoh, A. Furube, Y. Ohga, A. Shinpo, S. Suga, K. Sayama, H. Sugihara, H. Arakawa, *J. Phys. Chem. B* **2003**, *107*, 597.
[17] M. P. Brun, L. Bischoff, C. Garbay, *Angew. Chem. Int. Ed.* **2004**, *43*, 3432.
[18] L. Zhao, D. A. Loy, K. J. Shea, *J. Am. Chem. Soc.* **2006**, *128*, 14250.
[19] P. O. Jackson, M. O'Neill, W. L. Duffy, P. Hindmarsh, S. M. Kelly, G. J. Owen, *Chem. Mater.* **2001**, *13*, 694.
[20] M. Chen, K. P. Ghiggino, A. Launikonis, A. W. Mau, E. Rizzardo, W. H. Sasse, S. H. Thang, G. J. Wilson, *J. Mater. Chem.* **2003**, *13*, 2696.
[21] C. Kim, A. Trajkovska, J. U. Wallace, S. H. Chen, *Macromolecules* **2006**, *39*, 3817.
[22] Q. Fu, L. Cheng, Y. Zhang, W. Shi, *Polymer* **2008**, *49*, 4981.
[23] P. P. Wells, H. Morrison, *J. Am. Chem. Soc.* **1975**, *97*, 154.
[24] S. R. Trenor, A. R. Shultz, B. J. Love, T. E. Long, *Chem. Rev.* **2004**, *104*, 3059.
[25] B. Ren, D. Zhao, S. Liu, X. Liu, Z. Tong, *Macromolecules* **2007**, *40*, 4501.
[26] B. Kiskan, Y. Yagci, *J. Polym. Sci., Part A: Polym. Chem.* **2014**, *52*, 2911.
[27] J. Ling, M. Z. Rong, M. Q. Zhang, *J. Mater. Chem.* **2011**, *21*, 18373.
[28] P. Ferruti, *Ion-Chelating Polymers (Medical Applications)*, CRC Press Inc., Boca Raton, FL **1996**, p. 5/3334.
[29] P. Ferruti, M. A. Marchisio, R. Duncan, *Macromol. Rapid Commun.* **2002**, *23*, 332.
[30] P. Ferruti, S. Manzoni, S. C. Richardson, R. Duncan, N. G. Pattrick, R. Mendichi, M. Casolaro, *Macromolecules* **2000**, *33*, 7793.
[31] J. Franchini, E. Ranucci, P. Ferruti, M. Rossi, R. Cavalli, *Biomacromolecules* **2006**, *7*, 1215.
[32] B. V. Slaughter, S. S. Khurshid, O. Z. Fisher, A. Khademhosseini, N. A. Peppas, *Adv. Mater.* **2009**, *21*, 3307.
[33] L. Cai, J. Lu, V. Sheen, S. F. Wang, *Biomacromolecules* **2012**, *13*, 1663.
[34] L. Cai, J. Lu, V. Sheen, S. F. Wang, *Biomacromolecules* **2012**, *13*, 342.
[35] E. Jacchetti, E. Emilitri, S. Rodighiero, M. Indrieri, A. Gianfelice, C. Lenardi, A. Podestà, E. Ranucci, P. Ferruti, P. Milani, *J. Nanobiotechnol.* **2008**, *6*, 14.
[36] J. Shi, J. Ouyang, Q. Li, L. Wang, J. Wu, W. Zhong, M. M. Xing, *J. Mater. Chem.* **2012**, *22*, 23952.
[37] J. Ling, M. Z. Rong, M. Q. Zhang, *Polymer* **2012**, *53*, 2691.
[38] R. H. Kim, H. S. Shapiro, J. J. Li, J. L. Wrana, J. Sodek, *Matrix Biol.* **1994**, *14*, 31.
[39] C. Chun, H. J. Lim, K.-Y. Hong, K.-H. Park, S.-C. Song, *Biomaterials* **2009**, *30*, 6295.
[40] K. X. Wang, D. T. Denhardt, *Cytokine Growth Factor Rev.* **2008**, *19*, 333.
[41] R. Aschaffenburg, J. Mullen, *J. Dairy Res.* **1949**, *16*, 58.